J. Fluid Mech. (2005), *vol.* 525, *pp.* 355–379.
DOI: 10.1017/S0022112004002824 Printed in the United Kingdom

Viscosity ratio effects on the coalescence of two equal-sized drops in a two-dimensional linear flow

By YOSANG YOON[1], MARCOS BORRELL[1], C. CHARLES PARK[2] AND L. GARY LEAL[3]

[1]Department of Chemical Engineering, University of California at Santa Barbara, Santa Barbara, CA 93106-5080, USA

[2]Department of Mechanical Engineering, University of California at Santa Barbara, Santa Barbara, CA 93106-5080, USA

[3]Department of Chemical Engineering and Department of Materials, University of California at Santa Barbara, Santa Barbara, CA 93106-5080, USA

(Received 3 May 2004 and in revised form 8 October 2004)

The effect of the dispersed to continuous-phase viscosity ratio on the flow-induced coalescence of two equal-sized drops with clean interfaces was experimentally investigated. The experimental systems consisted of polybutadiene drops suspended in polydimethylsiloxane. The bulk-phase rheological properties of the fluids are Newtonian under the very weak flow conditions of the coalescence experiment (strain rate, $G < 0.08\,\mathrm{s}^{-1}$). Both head-on and glancing collisions were studied in a purely extensional flow (flow-type parameter, $\alpha = 1.0$) for the viscosity ratio (λ) range from $O(0.1)$ to $O(10)$. For head-on collisions, the dimensionless drainage times increased with the capillary number (Ca) as $Ca^{3/2}$ for all the viscosity ratios, which is consistent with theoretical predictions based on a simple film drainage model. The drainage time at a fixed Ca increased with the viscosity ratio and scaled as $\lambda^{0.82}$. In the case of glancing collisions, the critical coalescence conditions were examined by changing the initial offset, which results in different collision trajectories. In an earlier paper (Yang *et al.* 2001) that studied a system with a viscosity ratio of 0.096, the critical capillary number (Ca_c) for coalescence always decreased with the increasing offset. However, the present study shows that when the viscosity ratio is greater than $O(0.1)$, the critical capillary number decreases with increasing offset only for the smallest offsets, but then increases with increasing offset until a critical offset is reached above which coalescence is not observed. This is because coalescence for the larger offsets occurs in the extensional quadrant ($\phi > 45^\circ$) after the external flow has begun to pull the drops apart. At small offsets, drops coalesced in the compression quadrant with an orientation angle, $\phi < 45^\circ$. At the larger offsets, drops also coalesced in the compression quadrant for small Ca, but above some critical Ca, the coalescence angle jumped abruptly (i.e. with a very small change in Ca) to coalescence in the extensional quadrant. Coalescence with $\phi > 45^\circ$ is more prevalent for the higher viscosity ratio systems. On the other hand, the maximum offset for coalescence decreased with the viscosity ratio as expected.

1. Introduction

In many cases, blends of immiscible polymers consist of a dispersion of droplets of one polymer in a continuous suspending matrix of the other. It is important to understand and control the size and size distribution of the dispersed droplets because the properties of the blend depend on them. Commercial polymer blends are often formed in mixers such as blade-type batch mixers or twin-screw extruders. The fluid dynamics of the mixing process is extremely complicated. Although the size distribution is affected by the shear rate, flow type, surface tension, flow history, viscosity ratio, surfactant, and so on, the final drop size distribution is determined by a balance between flow-induced breakup and coalescence. Small drops are produced in regions of high deformation rate by breakup, whereas coalescence occurs in the regions of more gentle flow within the mixer (Milner & Xi 1996).

In spite of the importance of flow-induced coalescence in applications, our understanding of the process is still incomplete. There have been theoretical studies of the hydrodynamic interaction of drops, and the drainage, deformation and rupture of the thin film. The majority of this work has focused on numerical simulations of the interactions of two spherical/deformable drops in a flow (Wang, Zinchenko & Davis 1994; Loewenberg & Hinch 1997); the drainage of the thin film between two colliding drops within an asymptotic framework (Abid & Chesters 1994; Rother, Zinchenko & Davis 1997; Bazhlekov, Chesters & van de Vosse 2000; Rother & Davis 2001); and the three-dimensional problems of the collision and coalescence of two deformable drops (Loewenberg & Hinch 1997; Zinchenko, Rother & Davis 1997; Cristini, Blawzdziewicz & Loewenberg 2001). On the other hand, most of the experimental works are based on blending studies that analyse the drop size distribution of a full emulsion or blend (Vinckier *et al.* 1998; Lyu, Bates & Macosko 2000; Ramic *et al.* 2000; Burkhart *et al.* 2001; Hudson, Jamieson & Burkhart 2003). Until very recently, there were no experimental studies at the individual drop level of resolution. Trajectories of a pair of drops in either shear (Guido & Simeone 1998) or extensional flow (Tretheway, Muraoka & Leal 1999) had been studied, but coalescence was not observed owing to the relatively large drops that were studied. Hu, Pine & Leal (2000) initiated an investigation of the flow-induced coalescence of two equal-sized drops in a planar extensional flow using a miniaturized version of the four-roll mill so that the drop size could be reduced. They studied the coalescence of polybutadiene (PB) drops in a polydimethylsiloxane (PDMS) suspending fluid for both clean interfaces and surfactant (compatibilizer) systems. In a more comprehensive study, Yang *et al.* (2001), then reported experimental coalescence data for both head-on and glancing collisions for the clean interface system. The effects of different collision trajectories (corresponding to different initial offsets from a head-on collision) as well as the flow type were systematically examined for a single PB/PDMS with a viscosity ratio of 0.096. The data were compared with a simplified theoretical model based on the film drainage approximation of Chesters (1991). The effect of compatibilizer on the coalescence of two equal-sized drops was also studied by Hu *et al.* (2000) and Ha, Yoon & Leal (2003). The coalescence efficiency of two drops in a simple shear flow was also investigated by Mousa, Agterof & Mellema (2001).

In the present study, we experimentally investigate the effect of the dispersed to continuous-phase viscosity ratio on the flow-induced coalescence of two equal-sized drops with clean interfaces. Both head-on and glancing collisions were studied for a viscosity ratio range from $O(0.1)$ to $O(10)$. The collision or film drainage time, which is the period from the point when the centre-to-centre distance is equal to one undeformed drop diameter to the instant of coalescence, was measured for head-on

λ	Polymer	Viscosity (Pa s)	M_n	M_w/M_n	Interfacial tension (mN m^{-1})	Source
0.07	PB	2.16	6009	1.04	4.6	Polymer source
0.19	PB	5.5	5000	–	4.6	Aldrich
0.54	PB	15.9	13 400	1.03	4.6	Polymer source
1.2	PB	34	17 500	1.03	4.7	Polymer source
4.1	PB	120	21 700	1.05	4.9	Polymer source
6.8	PB	199	24 900	1.01	5.0	Polymer source
Suspending fluid	PDMS	29.3	103 400	1.65	–	United Chemical

TABLE 1. Experimental systems.

collisions. In the case of glancing collisions, the critical coalescence conditions were examined by changing the initial offset, which results in different collision trajectories. Although many aspects of the results are as yet difficult to explain, they point the way to further theoretical investigations of the coalescence process.

2. Experiment

2.1. *Experimental apparatus*

The coalescence experiment was carried out in a miniaturized version of the computer-controlled four-roll mill, that was originally developed by Bentley & Leal (1986) for studies of drop deformation and breakup. The range of strain rate, G, that can be generated in the current device is $10^{-4} \leqslant G \leqslant 4.7\,\mathrm{s}^{-1}$. The motions of the drops were viewed using a long focal length optical microscope ($\times 12$) and a CCD camera (768×494 pixel). The maximum resolution of the image is 0.719 μm/pixel. The captured images were sent to a PC equipped with a frame grabber board for real-time visualization. The details of the apparatus can be found in Yang *et al.* (2001).

2.2. *Experimental systems*

In the present study, six different viscosity ratio systems ($\lambda = 0.07, 0.19, 0.54, 1.2, 4.1$ and 6.8) were chosen to investigate the viscosity ratio effect on drop coalescence. Polydimethylsiloxane (PDMS, $M_n = 103\,400$, $M_w/M_n = 1.65$, $\mu = 29.3$ Pa s) was used as the suspending fluid for all the viscosity ratio systems, and six different molecular weights of polybutadiene (PB) were used as the drop to change the viscosity ratio, as shown in table 1. Although the densities (970 kg m^{-3} for PDMS and 895 kg m^{-3} for PB) are not well matched, the effects of buoyant forces are negligible because the diameter of the PB drops is less than 100 μm and the corresponding Bond numbers (Bo) for the experiment are very small ($Bo \sim O(10^{-4})$). The materials were used as received from the vendors without any treatment. The interfacial tension between the two phases was evaluated by measuring the drop deformation in a weak flow (linear deformation regime), using the small deformation theory of Taylor (1934). Although polymers of relatively large molecular weight were used, the fluids can be considered as Newtonian under the very weak flow conditions of the coalescence experiment (strain rate, $G < 0.08\,s^{-1}$).

2.3. *Experimental procedures*

A drop was made to a desired size outside the four-roll mill and injected into the flow cell. To control the drop size, a drop injection method was developed. The

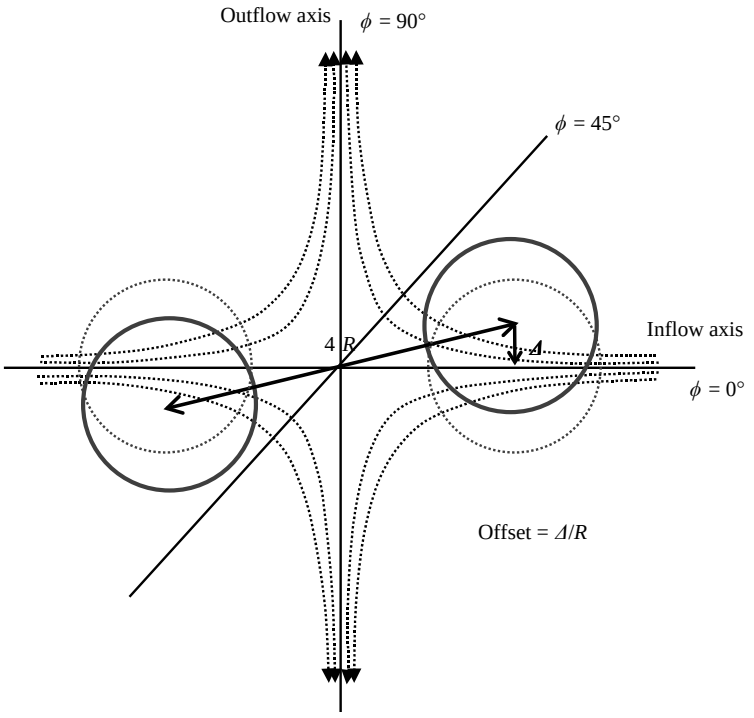

FIGURE 1. Schematic diagram of the flow field by a four-roll mill (the definitions of the coordinate system and the offset to the inflow axis).

injection system consists of an inner micro-sized needle (10 μm tip, World Precision Instruments, μTip^{TM}) and an outer capillary tube. When PB is extruded through the micro-sized tip into the outer capillary tube containing the suspending fluid (PDMS), the extruded PB thread breaks into a series of small equal-sized drops under the capillary induced motion. The drop sizes are controlled by the injection pressures of the drop (PB) and suspending fluid (PDMS). Several drops made in the injection system were injected from the capillary tube into the flow cell and then one drop was chosen to carry out the experiment. Two equal-sized drops were produced by stretching this drop in a planar extensional flow at a capillary number, Ca, slightly above the maximum value for steady-state deformation. Once the drop has reached a sufficient degree of stretch, the flow is stopped, and the drop breaks under the capillary induced motion. The formation of very small satellite drops between the two major drops is generally unavoidable. These small satellite drops were coalesced with one of the two major drops by gently reversing the flow. This process did not change the major drop size by a measurable amount. After establishing the initial positions along the symmetry axis of the four-roll mill, with their centres separated by two undeformed diameters, a certain offset was introduced and then a 'reversed' flow of a given strain rate and α was imposed on the two drops, as shown in figure 1.

When the drops are initially on the inflow axes (initial offset equal to zero), this leads to a head-on collision. The collision or film drainage time was measured, which is the period from the point when the centre-to-centre distance, scaled by the undeformed drop diameter, is 1 to the instant of coalescence. An active control algorithm was incorporated to prevent the drops from rotating away from the inflow axis. The control scheme uses very small changes in the flow type parameter, α, which

changes the inflow axis slightly while the shear rate remains constant, to maintain the orientation of the line of centres between drops at a fixed angle. This control scheme was verified to have no measurable effect on the film drainage time by Yang *et al.* (2001). The introduction of a non-zero offset from the inflow axes of the undisturbed flow leads to a glancing collision. Because the initial offset is a non-zero value, the drops rotate as they come together. There is a finite time available for film drainage before they are separated by the flow. Therefore, coalescence occurs only if the capillary number (Ca) is less than a critical capillary number (Ca_c). In the case of glancing collisions, the critical capillary number was determined at various initial offsets. For these glancing collisions, the drop size was fixed ($R = 27\,\mu\text{m}$), and the capillary number was varied by changing the strain rate of the flow. The trajectories of drops interacting in the flow and the collision time were also studied.

The experimental data for the drainage time (head-on) and the critical capillary number are reproducible to within about 5% in the worst case. The data for the coalescence angle versus the other parameters of the system are a little less reproducible, at something close to 8%. These estimates are the result of a non-systematic attempt by one of us to reproduce the data, but also represent the experience of new students as they try to reproduce the experimental results of an earlier student.

Finally, it is important to note that with the optics of the present experimental set-up, we are unable to resolve the thin film formed between the colliding drops at close contact.

3. Results and discussion

The hydrodynamic problem of two equal-sized drops colliding in a flow at very low Reynolds number can be characterized by dimensionless parameters,

$$Ca = \frac{G\mu_s R}{\sigma}, \quad \lambda = \frac{\mu_d}{\mu_s}, \quad \frac{\Delta}{R}, \quad \alpha, \quad \frac{h_c}{R}. \tag{3.1}$$

Ca is the capillary number, λ is the viscosity ratio of the drop to the suspending fluid, Δ/R is the initial offset (defined as the shortest distance from the centre of the drop to the inflow axis divided by drop radius R with the centre-to-centre distance of $4R$ as shown in figure 1) and α is the flow-type parameter defining the type of the imposed flow ($\alpha = 1.0$ for purely extensional flow and $\alpha = 0.0$ for simple shear flow). Lastly, in the final film-rupture stage, the Hamaker constant characterizing the strength of the van der Waals force can be associated with a critical film thickness that we have denoted as h_c/R.

Flow-induced coalescence has been modelled and described as consisting of three stages. The first stage is the approach and collision of drops. The second stage is the drainage of the thin film between the drops. During this stage, the drop surface deforms near the contact point. The deformation depends on the hydrodynamic force from the external flow that pushes the drops together relative to the capillary forces due to interfacial tension. As Ca increases, the tendency for the drops to deform during the collision process will increase; thus the extent of the deformed region increases, and the rate of film thinning decreases because the maximum pressure in the thin gap, which provides the pressure gradient that pushes the fluid out of the gap, is limited roughly to the capillary pressure. As the film thinning progresses, the distance between the two drops may become small enough for non-hydrodynamic attractive forces to induce an instability leading to film rupture. When this happens,

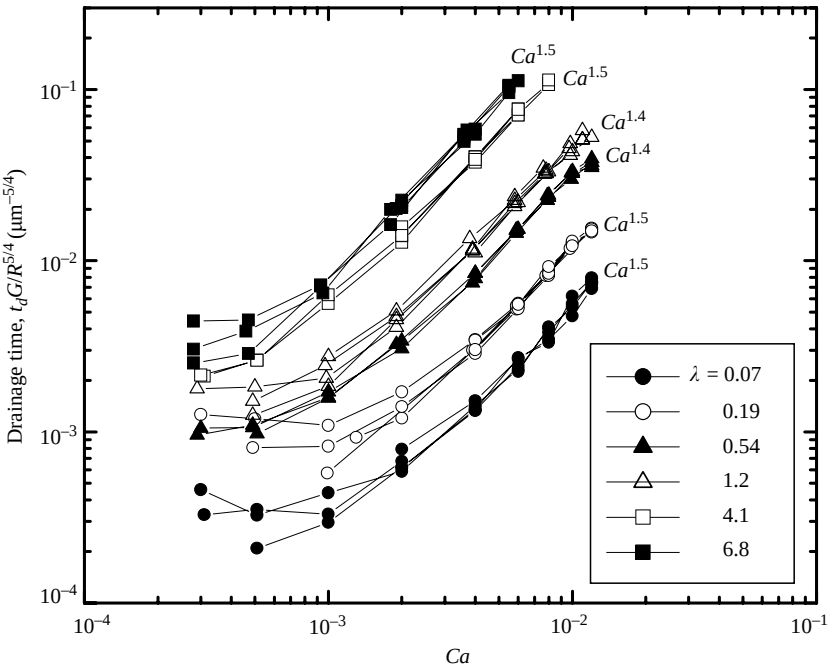

FIGURE 2. The scaled dimensionless drainage time as a function of Ca for head-on collisions in the flow of $\alpha = 1.0$ for the various viscosity ratios. The equations on the plot represent the power law fit of the data in the linear regime ($Ca > 0.004$ for $\lambda = 0.07, 0.19, 0.54, 1.2$ and $Ca > 0.002$ for $\lambda = 4.1, 6.8$).

the drops coalesce. Therefore, when the time available for the drainage process is finite, as in the case of a glancing collision, coalescence occurs only if Ca is less than a critical value (Ca_c). The duration of the third (rupture) stage is instantaneous compared to the two previous stages.

The collision of drops in a viscous fluid thus leads to coalescence only at small capillary numbers. The overall drop shape remains nearly spherical during the collision process, except for the local deformation described above in a local region around the point of contact. We have noted that the rate of film drainage depends on the capillary number. The rate of film drainage also strongly depends on the mobility of the interfaces during drop interaction. The interfacial mobility depends on the viscosity ratio for a clean interface system.

3.1. *Head-on collisions*

When the drops are initially on the inflow axes of the flow (with initial offset zero), the pair of drops does not rotate, and is pushed together under the action of the hydrodynamic force along the line of centres until they coalesce. Figure 2 shows the drainage time as a function of the capillary number for six different viscosity ratios. The drainage time is scaled with the undeformed drop radius, $R^{5/4}$. This scaling was empirically shown by Yang *et al.* (2001) to reduce drainage time data at fixed λ to a single universal line for a range of drop sizes, $R = 10 \sim 60\,\mu m$. In the present head-on experiments, the various curves in figure 2 at each value of the viscosity ratio represent data for different drop sizes, which varied between $R = 25 \sim 50\,\mu m$. The drainage time increases with the increase of the capillary number because the local deformation near the contact point increases. The transition to a plateau at lower

values of Ca is due to the increased relative contribution of the overall deformation of the drops to the film drainage process (Baldessari 2004). As the viscosity ratio is increased, the drainage time increases and the transition to a plateau occurs at decreased Ca.

The local velocity in the thin film region was analysed in the form

$$u = u_p + u_t \tag{3.2}$$

in the scaling theory of thin film drainage (Chesters 1991; Yang *et al.* 2001). Here, u_t is the uniform portion of the velocity profile due to the finite velocity at the 'mobile' interfaces and u_p is the parabolic part driven by the capillary pressure gradient. The two components u_t and u_p can be related by means of an approximation to the shear stress balance across the drop interface.

$$u_t \sim \frac{1}{\lambda} u_p \left(\frac{a}{h}\right), \tag{3.3}$$

where h and a are the thickness and the lateral extent of the draining film, respectively. As the viscosity ratio increases, interface mobility is reduced and u_t decreases. Thus, the drainage time increases with the increased viscosity ratio.

The equations in figure 2 represent the power law fit of the data in the high capillary number regime (linear regime). We can see that in this regime, the drainage time scales as $Ca^{3/2}$ for all the viscosity ratio systems. According to the scaling model of film drainage (Yang *et al.* 2001), the time required for the film to drain to a critical thickness, h_c, can be estimated as

$$t_d G \sim \lambda Ca^{3/2} \sqrt{f(\lambda)\alpha^{1/2}} \left(\frac{R}{h_c}\right). \tag{3.4}$$

Hence, the experimental results are qualitatively consistent with the predictions from the simple scaling model.

Figure 3 shows the drainage time as a function of the viscosity ratio at a fixed capillary number. For a given capillary number, flow type, drop size, and assuming that h_c is independent of the viscosity ratio, the drainage time is predicted to depend on the viscosity ratio as

$$t_d G \sim \lambda^{1.0} \tag{3.5}$$

without considering $f(\lambda)$, which is a very weak function of λ ($f(\lambda) \sim \lambda^{0.11}$). However, as shown in figure 3, the experimental result exhibits a weaker dependence on the viscosity ratio

$$t_d G \sim \lambda^{0.82 \pm 0.03} \tag{3.6}$$

than is predicted by the simple scaling arguments.

The explanation for this difference is unclear at the moment. However, changes in the viscosity ratio can influence a number of features that may change the drainage time. First, both the overall shape of the drop, and the shape of the deformed film drainage region will depend on the viscosity ratio. Hence, the initial film 'thickness' and the film profile will be different at the point of collision (i.e. the point where the centre-to-centre distance is 2 undeformed radii). Both of these changes will influence the film drainage time in ways that are not included in the simple scaling model that led to (3.4). Moreover, there are other possibilities. For example, in order to increase the viscosity ratio, the molecular weight of the PB (or drop) is increased. Therefore, if h_c decreases with the molecular weight of PB, the drainage time can show a weaker dependence. If there is slip at the polymer–polymer interface at the highest viscosity

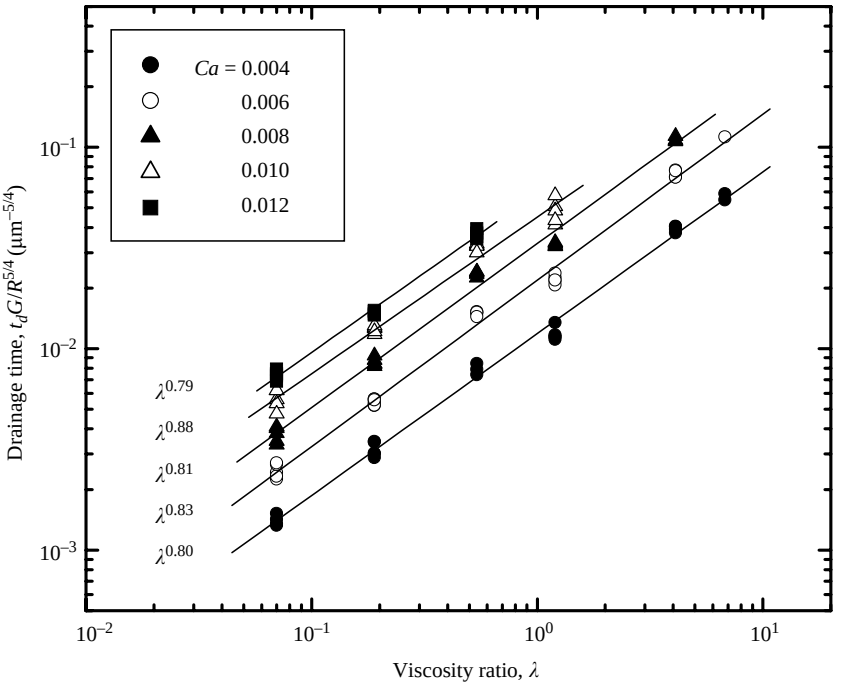

FIGURE 3. The scaled dimensionless drainage time as a function of the viscosity ratio at a fixed capillary number in the high capillary number regime (linear regime). The equations on the plot represent the power law fit of the data.

ratios, which is known to occur at polymer–polymer interfaces when the molecular weights are large enough (Goveas & Fredrickson 1998, 2000; Park, Baldessari & Leal 2003), the drainage time would also show a weaker dependence on λ. There may well be other mechanisms that we have not thought about. Until ongoing work is completed, we cannot distinguish between these various possibilities.

3.2. *Glancing collisions*

Head-on collisions rarely occur in practice. In reality, the head-on collision configuration is unstable, and even the smallest offset, or the smallest disturbance will lead to a glancing collision in the absence of the control algorithm that is used in the four-roll mill. As the drops come together in a glancing collision, they rotate owing to the initial offsets from the head-on collision trajectory. Therefore, the viscous force along the line of centres changes with time. Furthermore, there is a finite time available for film drainage before the force along the line of centres changes sign, and the drops are separated by the flow. As a consequence, a critical capillary number exists above which coalescence does not occur. The critical capillary number depends on the initial offset, the viscosity ratio, the drop size and the flow type.

3.2.1. *Viscosity ratio effect on coalescence for glancing collisions*

Figure 4 shows the trajectories of drops for the different viscosity ratios with a capillary number that is slightly greater than the critical capillary number for the initial offset of 0.08 ($\alpha = 1.0$, $R = 27\,\mu m$). The drops do not coalesce and are separated by the flow. Figure 4(a) shows the centre-to-centre distance scaled by the undeformed diameter and the orientation angle both plotted versus dimensionless time. Figure 4(b) shows the separation distance versus the orientation angle. As the

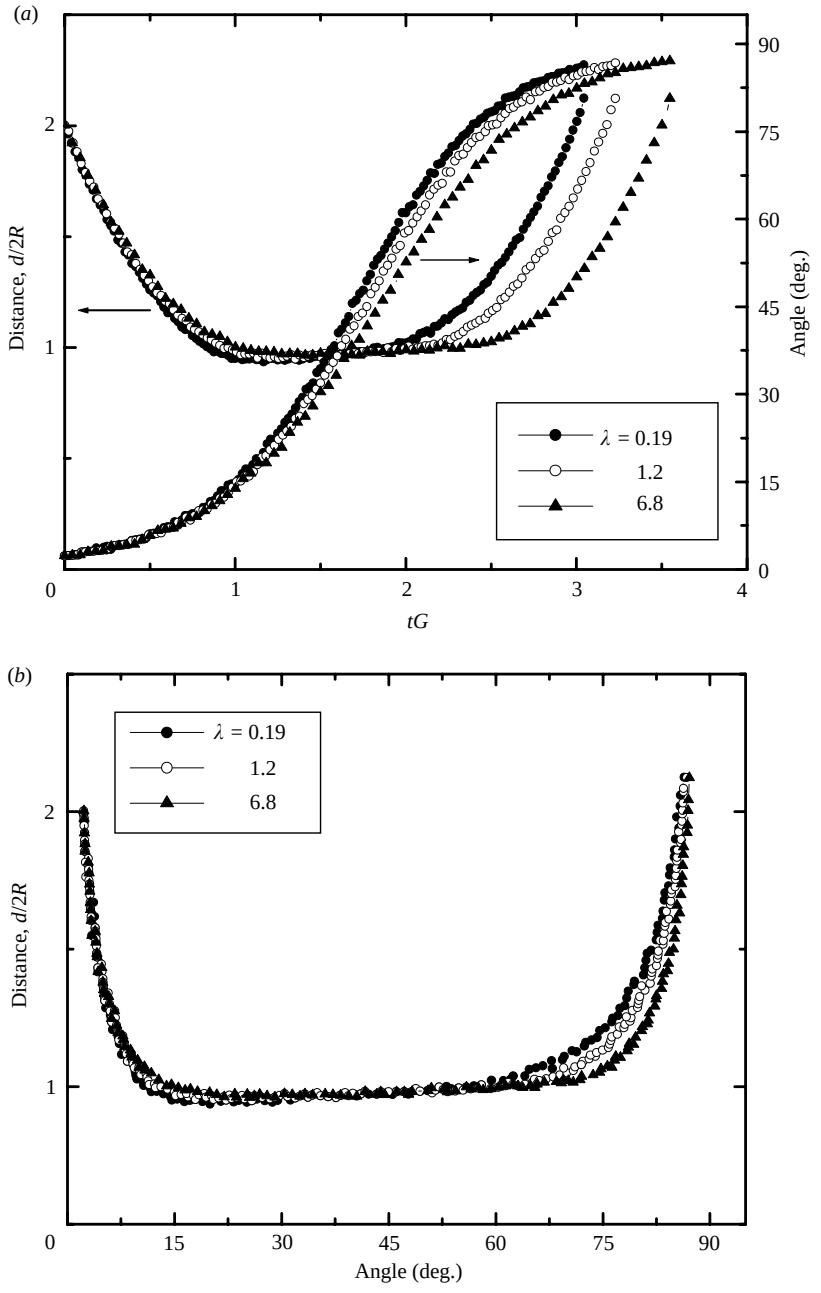

FIGURE 4. Trajectories of drops for the different viscosity ratios with a capillary number slightly greater than Ca_c at the offset of 0.08 ($\alpha = 1.0$, $R = 27\,\mu m$): data for $\lambda = 0.19$ at $Ca = 0.00721$ ($Ca_c = 0.00717$), $\lambda = 1.2$ at $Ca = 0.00417$ ($Ca_c = 0.00409$) and $\lambda = 6.8$ at $Ca = 0.00358$ ($Ca_c = 0.00354$): (*a*) separation distance and orientation angle versus dimensionless time; (*b*) separation distance versus orientation angle.

viscosity ratio increases, the drops rotate more slowly, and the point at which the drops noticeably separate is delayed to larger angles as shown in figure 4(*a*). The lubrication force in the thin film becomes stronger owing to the reduction of interfacial mobility

caused by increase of the viscosity ratio.† The increased lubrication force makes it more difficult for the drops to come into contact, and the drops also rotate to a larger angle before they separate significantly in order that the 'external' hydrodynamic force which pulls the drops apart becomes strong enough to overcome the enhanced lubrication force. Therefore, the trajectories of the distance versus orientation angle become more symmetric with the increased viscosity ratio, as shown in figure 4(*b*).

Figure 5 shows the trajectories of the drops for different initial offsets with a capillary number that is slightly greater than the critical capillary number for a viscosity ratio of 1.2 ($\alpha = 1.0$, $R = 27\,\mu\text{m}$). As the initial offset increases, the drops rotate more quickly and the available contact time for film drainage decreases as shown in figure 5(*a*). If we examine figure 5(*b*), we see that the approaching parts of the trajectories are different from each other owing to the different initial offsets. However, after the drops come into contact, it can be seen that they follow the same trajectories of separation distance versus angle. We have no explanation for this.

The drops rotate more quickly and the available contact time for thin-film drainage decreases with increased initial offset, as shown in figure 5. Therefore, we should expect that the critical capillary number for coalescence will decrease with increasing offset, and this is precisely what was found in our earlier study (Yang *et al.* 2001), where the viscosity ratio was 0.096. Thus, an extremely surprising observation from the present work is that the critical capillary number generally decreases with increased offset for small offsets, but then increases with further increase of the offset for all viscosity ratios greater than $O(0.1)$. Figure 6 shows the critical capillary number as a function of the initial offset in a planar extensional flow ($\alpha = 1.0$) for the various viscosity ratios ($\lambda = 0.19, 0.54, 1.2, 6.8$) and $R = 27\,\mu\text{m}$ (We plot data for both positive and negative offsets, though in this case of the pure straining flow ($\alpha = 1$), the data was actually measured for either a positive or negative offset and then the mirror-image point was added to the figure). The critical capillary number initially decreases with increased offset and there is a maximum offset beyond which coalescence is not possible, as we would expect. However, when the offset is greater than a certain value, the critical capillary number begins to increase with further increase of the offset.

We shall see shortly that this apparently surprising observation is due to the drops beginning to coalesce in the extensional quadrant of the flow (above the orientation angle of 45°, $\phi > 45°$). When the line of centres of the two drops rotates past 45°, the hydrodynamic force along the line of centres, created by the external flow, changes sign from a force that pushes the drops together to one that tends to pull the drops apart. Thus, the drops at the higher values of offset (and capillary number) coalesce while they are being pulled apart in the flow.

To explore the details of this, we next consider data for the coalescence angle as a function of the capillary number for the various viscosity ratio systems. We begin with the lowest viscosity ratio system in this study, $\lambda = 0.19$. Figure 7 shows the coalescence angle as a function of Ca for various initial offsets. As the capillary number increases, the coalescence angle increases. The critical capillary number for each offset (plotted in figure 6), corresponds to the data point at the right-hand end of each curve. We shall denote the angle at this capillary number as the critical coalescence angle. As the offset increases, the critical coalescence angle increases, but,

† The words 'interfacial mobility' are sometimes used to describe the strength of the reduction of interface velocity due to Marangoni effects in the presence of surfactant. In the present system, there is no surfactant present and we simply refer to the reduction in the scaled velocity at the interface of the thin film due to increased viscosity ratio.

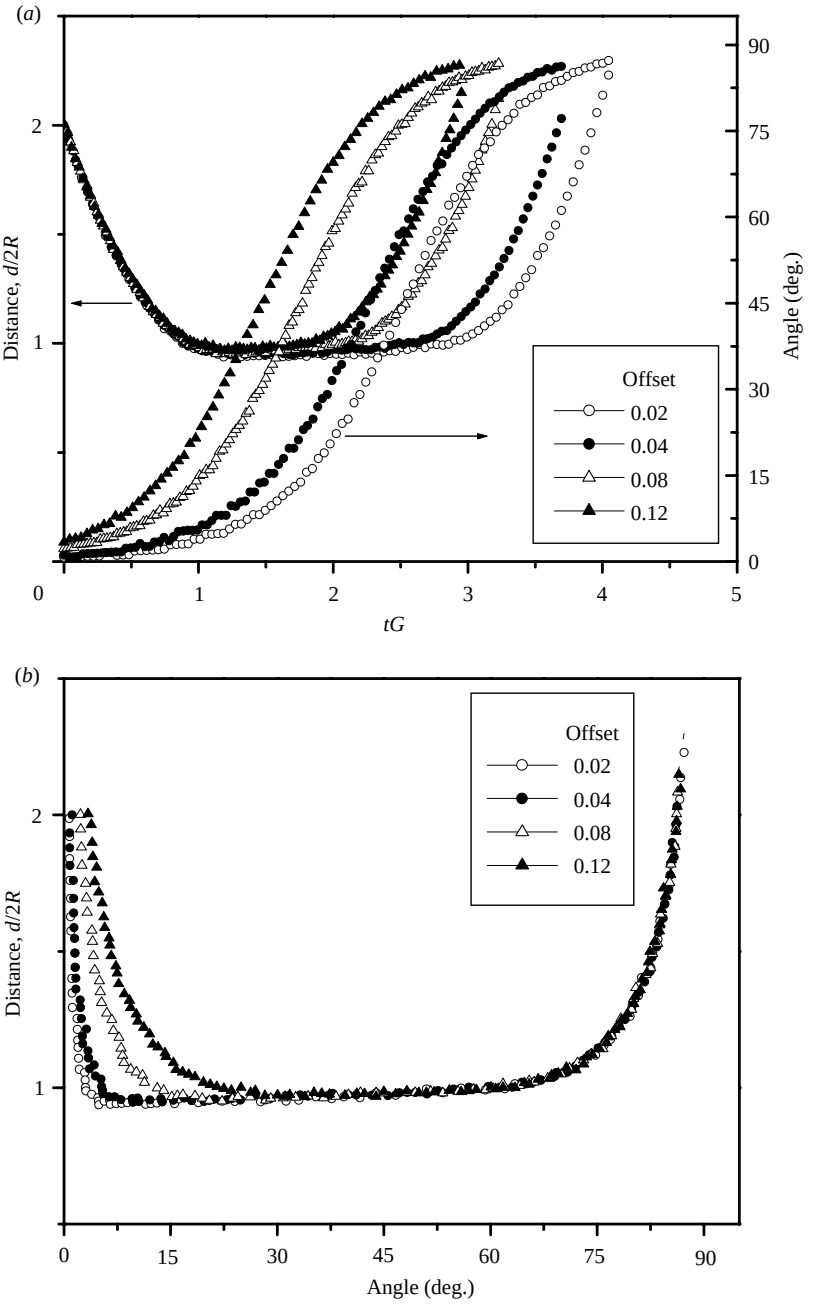

FIGURE 5. Trajectories of drops for the different initial offsets with a capillary number slightly greater than Ca_c ($\alpha = 1.0$, $\lambda = 1.2$, $R = 27\,\mu m$): data for offset = 0.02 at $Ca = 0.00497$ ($Ca_c = 0.00489$), offset = 0.04 at $Ca = 0.00401$ ($Ca_c = 0.00393$), offset = 0.08 at $Ca = 0.00417$ ($Ca_c = 0.00409$) and offset = 0.12 at $Ca = 0.00481$ ($Ca_c = 0.00477$): (*a*) separation distance and orientation angle versus dimensionless time; (*b*) separation distance versus orientation angle.

in this case, it only exceeds 45° for the very highest offset, 0.14, where the orientation angle becomes slightly larger than 45° and the drops can coalesce in the extensional quadrant ($\phi > 45°$) of the flow.

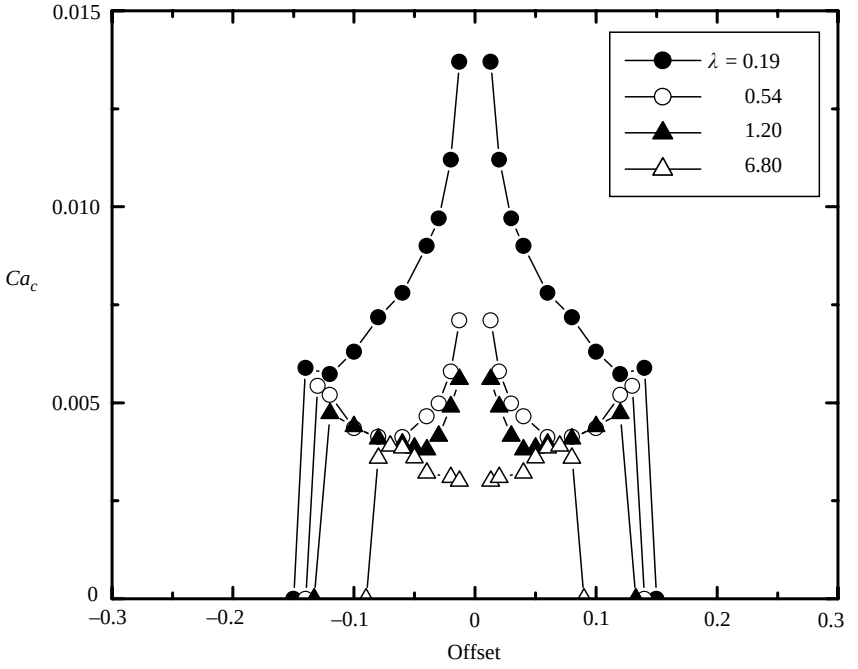

FIGURE 6. Critical capillary numbers as a function of the initial offset for the various viscosity ratios ($\alpha = 1.0$, $R = 27\,\mu$m).

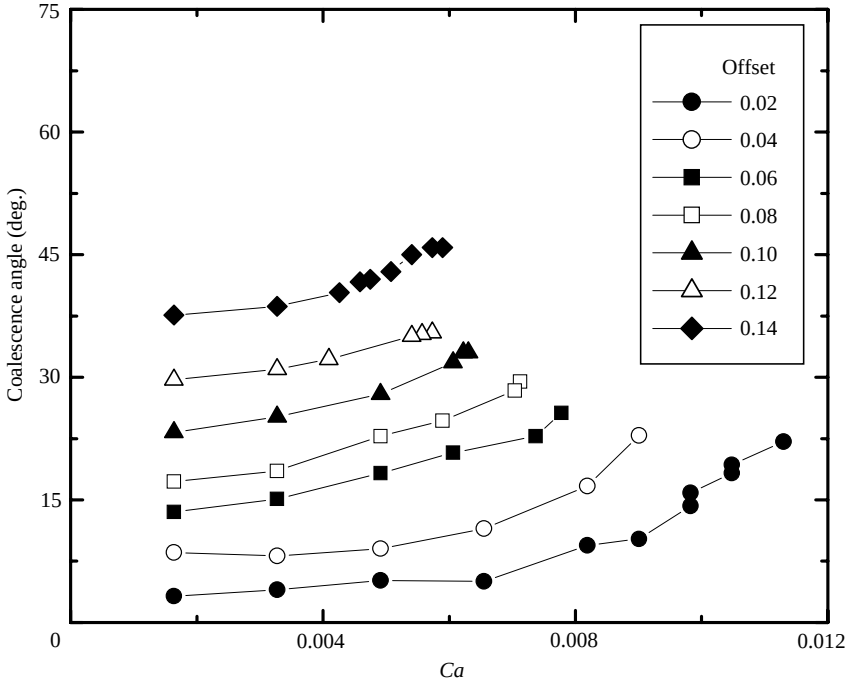

FIGURE 7. Coalescence angle as a function of the capillary number for $\lambda = 0.19$ ($\alpha = 1.0$, $R = 27\,\mu$m).

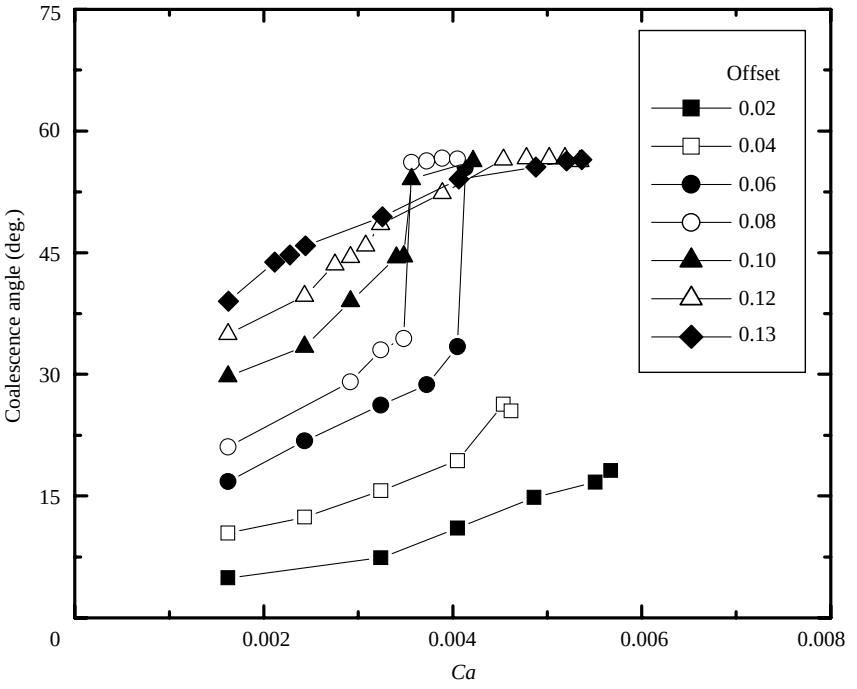

FIGURE 8. Coalescence angle as a function of the capillary number for $\lambda = 0.54$ ($\alpha = 1.0$, $R = 27\,\mu\text{m}$).

Figure 8 shows the same plot for a viscosity ratio of 0.54. The coalescence angle dependence on *Ca* is fundamentally different from that of the lower viscosity ratio system ($\lambda = 0.19$). At the smallest offsets (0.02 and 0.04), the coalescence angle increases with *Ca*, much like the previous case, but always remains small, $\phi \leqslant 23^\circ$. However, when the offset is between 0.06 and 0.1, the coalescence angle increases with *Ca* as before, but now when the capillary number reaches what one would anticipate to be its 'critical' value, there is a step change to coalescence in the extensional quadrant ($\phi > 45^\circ$) and the range of capillary numbers where the drops coalesce is increased. With only a very tiny increase of *Ca*, the coalescence angle changes from around 30° in the 'compressional' quadrant, to an angle of approximately 55° in the extensional quadrant. At the largest offsets (0.12, 0.13), the coalescence angle increases continuously up to 55° as *Ca* increases. In all cases, the critical capillary number is increased by the transition to coalescence in the extensional quadrant.

This tendency to coalesce in the extensional quadrant is further enhanced by increase of the viscosity ratio. The coalescence angles as a function of *Ca* for the more viscous systems, with viscosity ratios of 1.2 and 6.8, are shown in figures 9 and 10, respectively. The case $\lambda = 1.2$ shows behaviour that is very similar to the case $\lambda = 0.54$. The step change of the coalescence angle sets in at a slightly smaller offset and the coalescence angle in the extensional quadrant is increased to approximately 60°, but otherwise things are very similar. For the viscosity ratio of 6.8, there is a transition to coalescence in the extensional quadrant for all offsets $\geqslant 0.02$, as shown in figure 10. The maximum coalescence angle in the extensional quadrant is again increased to approximately 68°.

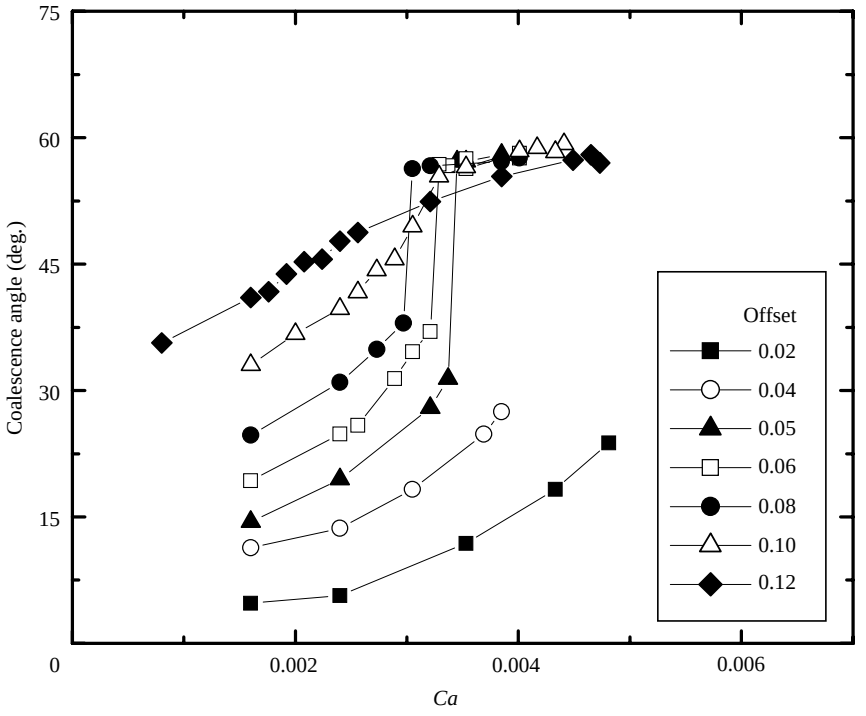

FIGURE 9. Coalescence angle as a function of the capillary number for $\lambda = 1.2$ ($\alpha = 1.0$, $R = 27\,\mu$m).

The possibility of coalescence occurring either at relatively small angles, or at angles beyond the point where the flow is acting to pull the drops apart is already anticipated, at least qualitatively, by the theoretical studies of Rother *et al.* (1997, 2001). Although the detailed problems studied were somewhat different from the planar homogeneous flows studied here, these authors show that the film thickness during a collision can have two minima as the film undergoes a transition from a dimpled configuration during the early part of the collision to a configuration with the minimum film thickness occurring at the nose of the drops later in the collision (when the force along the line of centres is reduced). In some cases, this second minimum occurred for angles that were slightly past the point when the force along the line of centres changes sign. It should be noted, however, that the second minimum was never the absolute minimum for the case shown explicitly in their paper and there are other aspects of the experiments, such as the role of the viscosity ratio that do not seem to be encompassed in any obvious way by a 'simple' transition from dimpled to an 'undeformed' film shape.

We believe that it is possible that the lack of coalescence in the compression quadrant, except for relatively small angles, is because the film thickness exhibits an absolute minimum at the rim during the early part of the collision, as Rother *et al.*'s solutions suggest. We speculate that the abrupt transition to coalescence with $\phi > 45^\circ$ requires some additional deformation beyond the transition to an 'undeformed' drop shape. As the viscosity ratio increases, the lubrication force in the thin film becomes stronger owing to the reduced interfacial mobility. We have seen in the trajectory measurements, that measurable separation of the drops is thereby retarded. The force

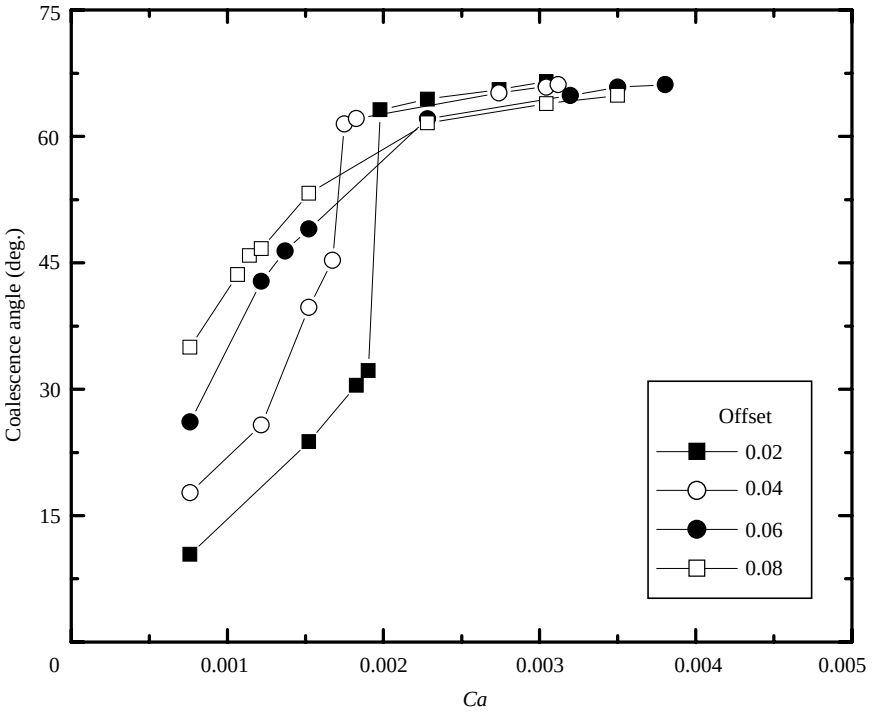

FIGURE 10. Coalescence angle as a function of the capillary number for $\lambda = 6.8$ ($\alpha = 1.0$, $R = 27\,\mu\text{m}$).

from the external flow that pulls the drops apart must become strong enough to overcome the enhanced lubrication force. The hydrodynamic force which pulls the drops apart is at first very small, but increases as the pair of drops rotate through the extensional quadrant. As this force increases, the suction pressure in the thin film, owing to the lubrication force, will also increase, provided the drops remain close together. If the force required to pull the drops apart is large enough, the suction pressure will become comparable to the capillary pressure, and the drops will begin to deform locally, forming a nipple-like region of higher curvature at the line of centres between the drops. Depending on the magnitude of this deformation, it may bring the drop interfaces close enough together at the line of centres to allow a sufficiently strong attraction due to van der Waals forces, to trigger film rupture and coalescence. The fact that coalescence with $\phi > 45^\circ$ occurs more readily for the higher viscosity ratio systems would seem to be qualitatively consistent with an explanation in terms of nipple formation in the thin-film region. Whether this mechanism works at any given viscosity ratio depends in a complicated way on how much deformation is necessary once ϕ reaches 45° (and the force along the line of centres changes sign) for the film thickness locally to reach the critical value $h_c$where van der Waals forces become strong enough to trigger film rupture. The amount of deformation that is possible depends on the 'initial shape' of the film at $\phi = 45^\circ$, including the mean film thickness. Together with the viscosity ratio, the latter quantity determines how large the suction pressure will become, and how quickly the drops separate. This, in turn,

determines whether the suction pressure reaches the point where the deformation is locally large enough to achieve h_c.†

As an example, let us consider the data for $\lambda = 1.2$ in figure 9, under the assumption that nipple formation is the main mechanism for the coalescence in the extensional quadrant. When the initial offset is small, the drops collide forcefully, and the thin film between the drops will become more dimpled as Ca increases. The critical coalescence angle is much less than 45° for the small offsets of 0.02 and 0.04. Furthermore, for these offsets, a small increase of Ca above Ca_c does not result in coalescence either for the orientation angles $30° < \phi < 45°$, or in the extensional quadrant. This means that the minimum film thickness (or at least the most unstable film configuration) for these cases is achieved early in the collision process, and the film thickness for angles between $\phi = 30°$ and 45° is larger than the critical film thickness, h_c, even though the force along the line of centres remains positive. Furthermore, if there is a secondary minimum in the film thickness in the extensional quadrant owing to the nipple formation, it does not reach the critical thickness for these cases. In contrast, when the initial offset is increased, the drops collide more gently (the force along the line of centres is decreased as the initial collision angle increases) than in the case of a smaller initial offset. The largest coalescence angle for $\phi < 45°$ increases with the offset. The critical film thickness can be reached at an angle closer to 45°. A small increase of Ca above the largest Ca at which coalescence occurs with $\phi < 45°$, results in coalescence in the extensional quadrant because a smaller deformation is required for the film thickness associated with nipple formation to reach the critical film thickness.

So far, we have suggested that the data can be explained based upon a deterministic evolution of film shapes during the drainage process, which we suppose leads to a minimum film thickness for $\phi < 45°$, and the possibility of nipple formation for $\phi > 45°$. However, a more commonly held view is that the rupture process is actually triggered by a thin-film instability at a point in the drainage process where the deterministic evolution of the film would not have led to a critical film thickness. We are skeptical of the applicability of the existing analyses of thin-film instability because they are developed based upon relatively crude approximations of the 'base state', i.e. approximations of the geometry (uniform thickness) and flow within the draining thin film. Nevertheless, it is worth considering the basic ideas, and whether they might apply to the present situation. Thin-film instability is initiated by hydrodynamic perturbations or thermal fluctuations, which lead to corrugation of the film surfaces (Manev, Scheludk & Exerowa 1974), which can grow in the presence of attractive van der Waals forces as the film thins (Sharma & Ruckenstein 1987, 1988). Thus, the processes of film thinning and the growth of the amplitude of the surface waves must be considered together. Generally speaking, the elasticity and the viscosity of the film interfaces and the viscosity of the bulk phases damp the growth rate of the perturbations. On the other hand, the perturbation growth rate increases with an increase of the viscosity ratio (Yeo & Matar 2003). It seems possible that the

† A possible alternative explanation has been suggested by one of the referees. This is based upon the idea that drainage may have progressed far enough during the compression part of the flow so that van der Waals forces produce film thinning (and eventually rupture) during the extensional part of the flow. We do not believe that this is the correct explanation. For example, it does not seem to be consistent with the observation that this effect is enhanced by increase of the viscosity ratio. However, until theoretical results are available to explore the mechanism in more detail, we cannot prove our point and we thus include this mention of the referee's idea.

two interfaces of the thin film could become closer in the extensional quadrant even though the force along the line of centres is pulling them apart, owing to the growing amplitude of the perturbations, rather than the 'deterministic' growth of a nipple-shaped region due to lubrication forces as suggested earlier. The fact that coalescence at $\phi > 45^\circ$ is favoured by larger viscosity ratios might then seem to be a consequence of the drops remaining 'in contact' for a longer period of time, and thus allow a longer period of time for the thin-film instability to grow.

In spite of the fact that thin film instability does seem to provide a reasonable qualitative explanation of many of the observed facts for these clean interface systems, it does not seem consistent with our earlier observations of systems with surfactant. According to the study of Ha *et al.* (2003), the presence of a surfactant also causes the drops to coalesce in the extensional quadrant. The presence of surfactant presumably decreases the mobility of the interfaces owing to Marangoni stresses, similarly to increasing the viscosity ratio. On the other hand, the presence of the surfactant at the interfaces is known to stabilize the film (decreasing the perturbation amplitude and retarding the growth of the instability) owing to the flow-induced redistribution of the surfactant (Yeo & Matar 2003). This suggests that thin-film instability is not the main mechanism for coalescence in the extensional quadrant in the presence of surfactants, and thus it seems unlikely to be the main mechanism for clean interface systems either.

The simple scaling theory of Chesters (1991), which we used in our earlier study (Yang *et al.* 2001), assumes that the draining film is a flat disk-like region between the drops, whose radius is determined by a quasi-steady force balance between the lubrication forces in the thin film, and the hydrodynamic force along the line of centres due to the external flow. In this model, the film thins continuously in time up to the point where the force along the line of centres changes sign and the angle of coalescence at the critical capillary number must be 45°. However, we have seen that the drops do not typically coalesce at this angle when $Ca = Ca_c$. The coalescence angle at Ca_c depends strongly on the viscosity ratio and the initial offset. Figure 11 shows the results for the critical coalescence angle as a function of the offset. With the exception of the largest offset values for $\lambda = 0.19$, the critical coalescence angle is always either quite small ($<30^\circ$), or it is significantly greater than 45°. As suggested earlier, the limitation to relatively small angles when coalescence occurs with $\phi \leqslant 45^\circ$ is most probably indicative of the fact that the evolution of film shapes is very complicated when the force driving this process (the force along the line of centres from the external flow) is time-dependent. It is also notable that the critical coalesce angle becomes independent of the offset once the drops start to coalesce in the extensional quadrant. In this regime, it is only the viscosity ratio that (apparently) determines the critical coalescence angle. In view of the apparent complexity of the process that we believe leads to coalescence during this part of the collision, this is a surprising result.

Figure 12 shows a comparison, for $\lambda = 1.2$, between the measured Ca_c (represented by circles) that reproduce the data in figure 6, and the Ca (represented by the triangles) at which the coalescence angle jumps into the extensional quadrant (note that this is also the largest capillary number at which coalescence occurs with $\phi < 45^\circ$). The difference between these two values of the capillary number increases with the offset. It should not be surprising that the shape of the curve for the largest capillary number where coalescence still occurs for $\phi < 45^\circ$ is qualitatively similar to what would be expected for the critical capillary number using the simple scaling theory. Although the orientation angles for these 'jump' values of Ca are not 45°, the drops rotate

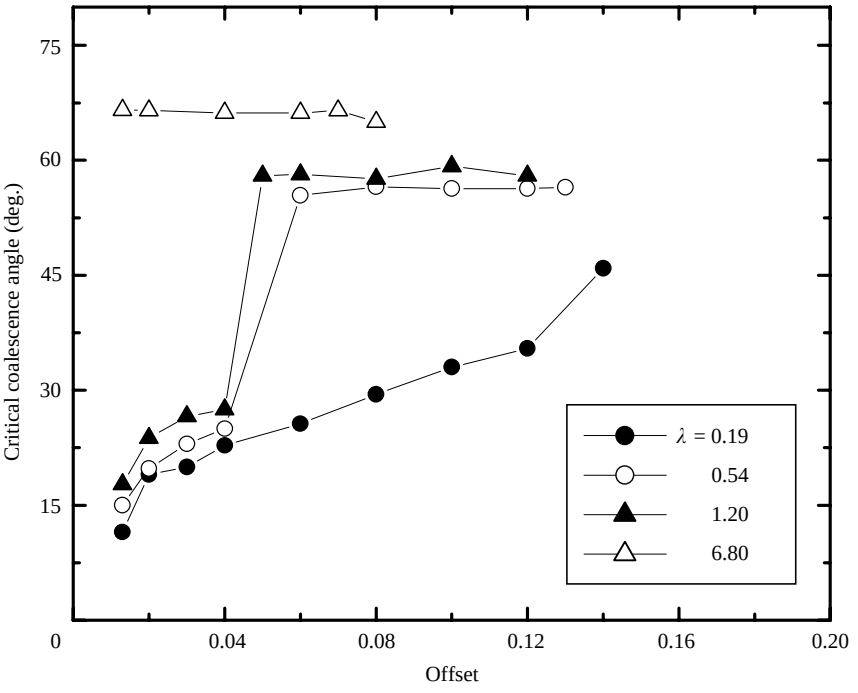

FIGURE 11. Critical coalescence angle (coalescence angles at Ca_c) versus initial offset for the various viscosity ratios ($\alpha = 1.0$, $R = 27\,\mu$m).

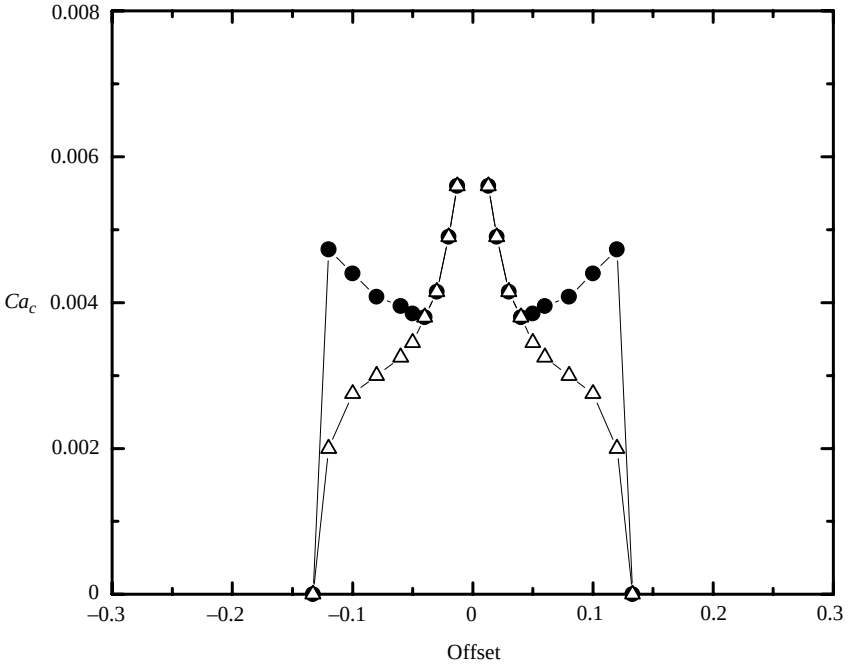

FIGURE 12. Comparison between ●, Ca_c and △, Ca_{jump} at which the coalescence angle jumps into the extensional quadrant or the largest Ca at which coalescence occurs with $\phi < 45^\circ$ for $\lambda = 1.2$ ($\alpha = 1.0$, $R = 27\,\mu$m).

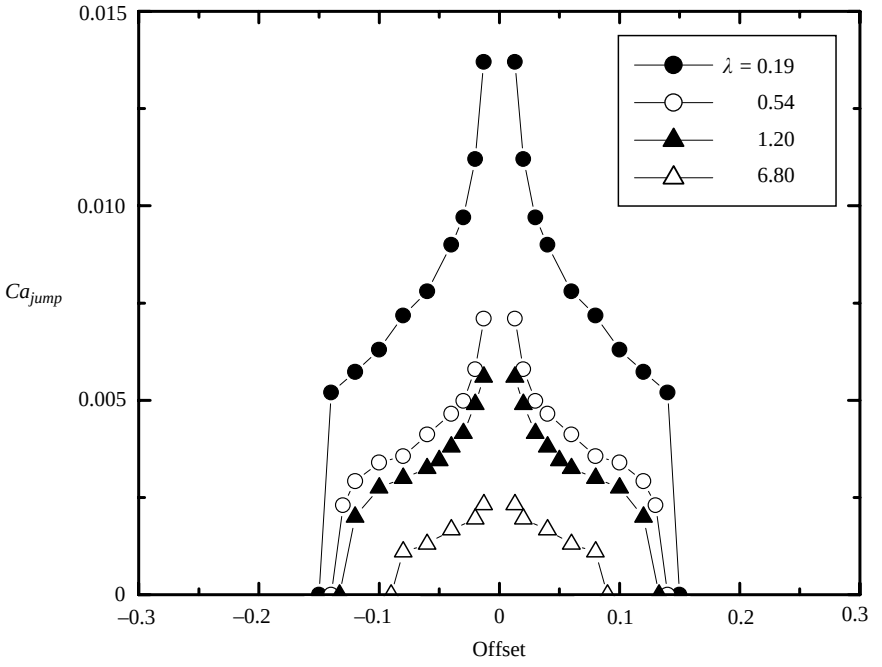

FIGURE 13. Jump capillary number (or the largest capillary number at which coalescence occurs with $\phi < 45°$) as a function of the initial offset ($\alpha = 1.0$, $R = 27\,\mu m$).

rapidly once ϕ is greater than $25° \sim 30°$, and the incremental change in Ca that would occur if the 'jump' occurred at 45° is small. The data in figure 12 simply emphasize the fact that the increase in Ca_c with increased offset that was observed in figure 6 is a result of the appearance of a new mechanism for coalescence that allows for coalescence with $\phi > 45°$.

Figure 13 shows the jump capillary number (or the largest capillary number at which coalescence occurs with $\phi < 45°$) as a function of the initial offset for all four of the viscosity ratios that are considered in this study. Again, the dependence of the jump capillary number on offset and viscosity ratio is similar to what would be expected for the critical capillary number according to the simple scaling theory.

Finally, another useful way to present the data that clearly illustrates the effect of changes in the viscosity ratio on the coalescence angle and the drainage time is shown in figures 14 and 15, for two fixed values of the offset equal to 0.04 and 0.08, respectively. As the viscosity ratio increases, the drainage time required for coalescence increases, and thus the coalescence angle also increases as previously discussed. Again, the interesting result is that the drops can coalesce with $\phi > 45°$, for both values of the offset for $\lambda = 6.8$, and for the larger offset for $\lambda = 0.54$ and 1.2.

3.2.2. *The dependence of Ca_c on the viscosity ratio*

Figure 16 shows the critical capillary number dependence on the viscosity ratio for the various initial offsets. Based upon the simple scaling theory, and the earlier data of Hu *et al.* (2000), we might have expected a simple power-law dependence of Ca_c on λ. Clearly, the data in figure 16 do not follow any such dependence. We have already indicated that the scaling theory is qualitatively flawed, so there is no surprise that our data do not follow its predictions. Furthermore, if we go back and look at the data plotted in the form shown in figure 6, it is clear that there cannot be any such

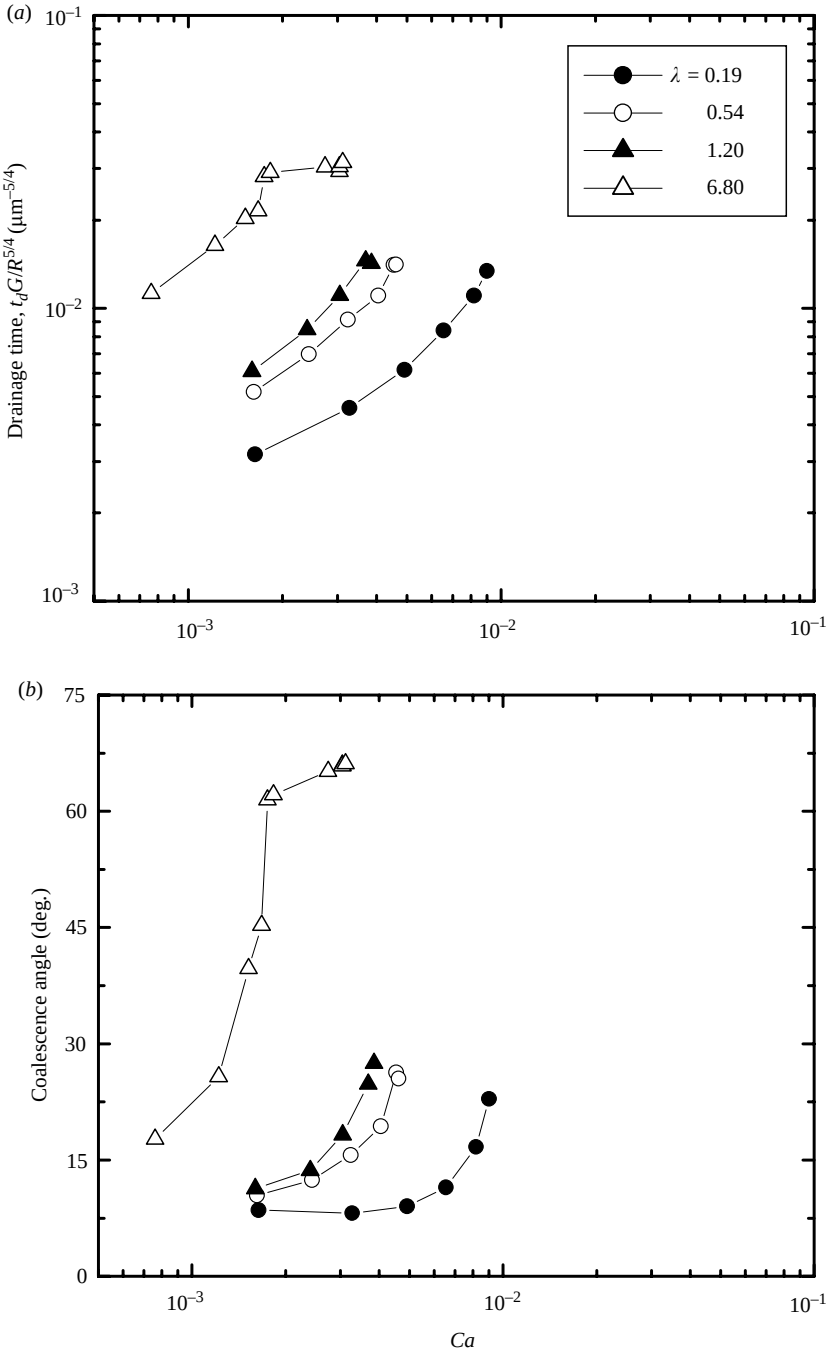

FIGURE 14. (*a*) Scaled dimensionless drainage time as a function of Ca and (*b*) coalescence angle as a function of Ca for the various viscosity ratios at the offset of 0.04 ($\alpha = 1.0$, $R = 27\,\mu m$).

power-law dependence in general. Obviously, the dependence of Ca_c on λ depends entirely on what value of the offset we choose. Hu *et al.* (2000) reported that there was an apparent power-law dependence of Ca_c on the viscosity ratio ($Ca \sim \lambda^{-0.41}$),

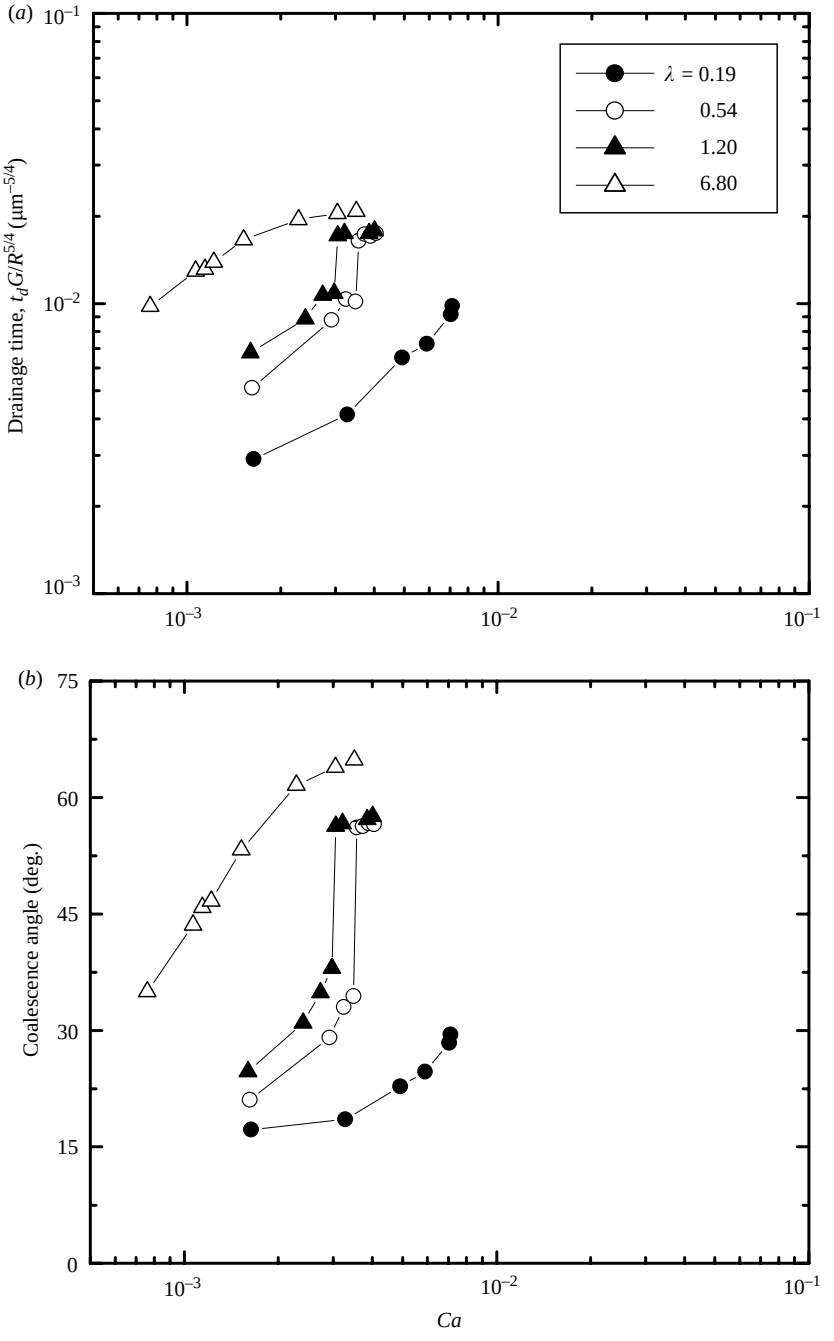

FIGURE 15. (*a*) Scaled dimensionless drainage time as a function of Ca and (*b*) coalescence angle as a function of Ca for the various viscosity ratios at the offset of 0.08 ($\alpha = 1.0$, $R = 27\,\mu$m).

but they only made measurements at a single fixed value of the offset (0.038). It was not anticipated at that time that the dependence on offset would be so complex, and it was thus believed that the power-law scaling they had found would apply independently of the offset. Clearly in view of what we know now, this is not the case.

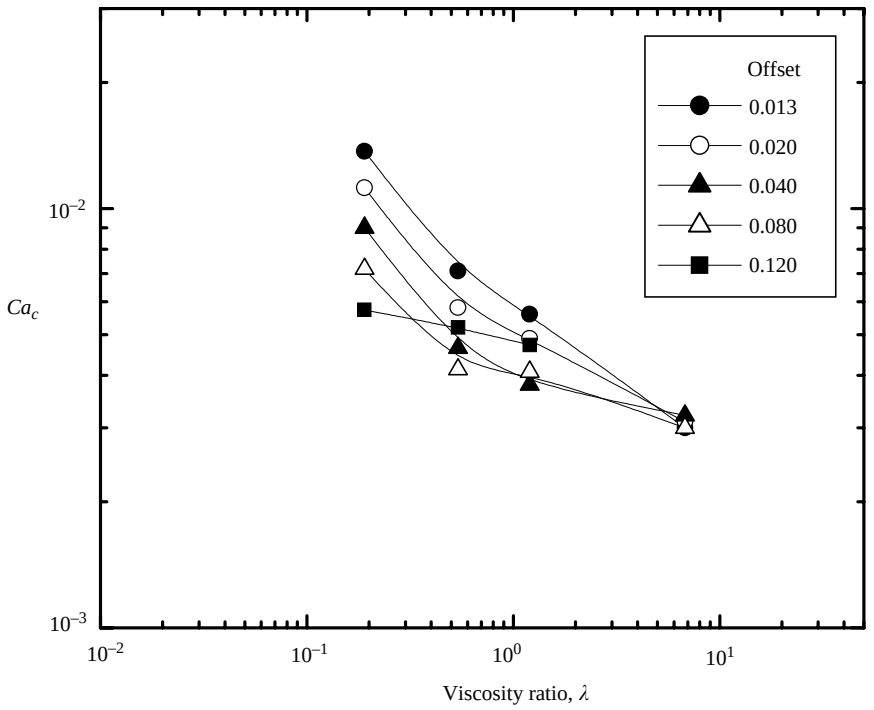

FIGURE 16. Critical capillary number as a function of the viscosity ratio at the various initial offsets ($\alpha = 1.0$, $R = 27\,\mu$m).

The lack of any power-law dependence of the critical capillary number on the viscosity ratio is at least partly because drops can coalesce with $\phi > 45^\circ$, as mentioned previously. Thus, in view of the results already shown in figures 12 and 13, we might anticipate that the maximum capillary number where coalescence occurs with $\phi < 45^\circ$ (i.e. the same quantity as plotted in figure 13) might show such a scaling dependence. We plot this value of the capillary number for the various offsets in figure 17. The inserted plot shows a comparison between the critical Ca_c (solid triangles) and the Ca mentioned above (open triangles) for an offset of 0.08. The capillary number plotted in figure 17 decreases linearly with increase of the viscosity ratio, following a linear power law. The average of the slopes is -0.48 ($Ca_{max,\phi<45^\circ} \sim \lambda^{-0.48}$). This dependence on the viscosity ratio is weaker than predicted for Ca_c by the simple scaling theory ($Ca_c \sim \lambda^{-2/3}$). Of course, the capillary number plotted in figure 17 is not Ca_c, but the largest Ca for which coalescence occurs with $\phi < 45^\circ$ as previously shown in figure 13.

4. Conclusions

The coalescence of two equal-sized drops in a linear flow has been experimentally investigated using a four-roll mill. The quantitative experimental data for the effect of the viscosity ratio on the coalescence at the individual drop level of resolution were provided.

For head-on collisions, the drainage times increased with the capillary number as $Ca^{3/2}$ for all the viscosity ratios, which is consistent with predictions from Yang *et al.* (2001) based on the simple scaling theory. The drainage time at a fixed Ca increased

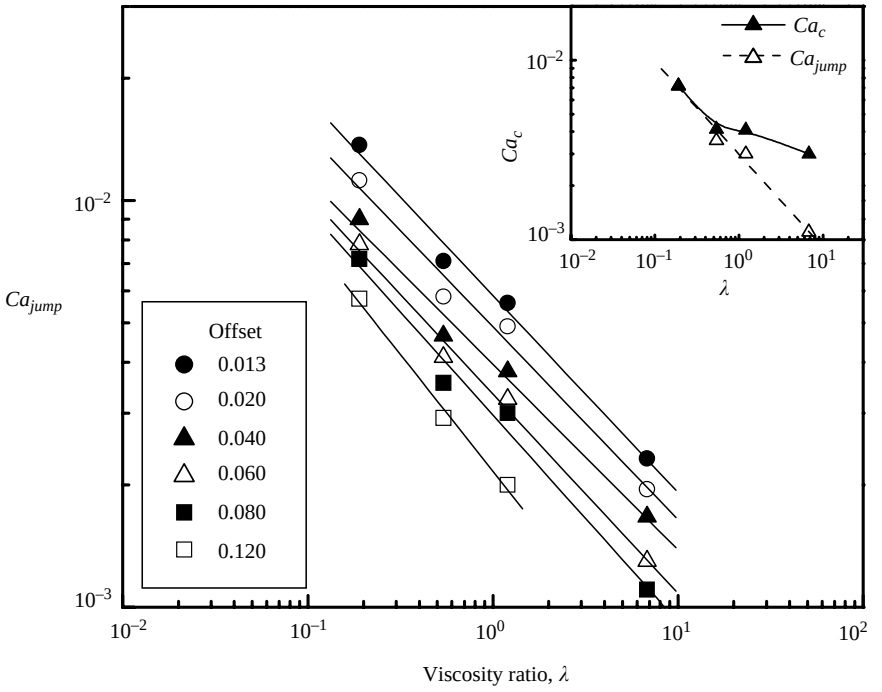

FIGURE 17. Jump capillary numbers (Ca_{jump}) as a function of the viscosity ratio at the various initial offsets. The average of the slopes is -0.48 ($Ca_{jump} \sim \lambda^{-0.48}$) by the power law fit of the data. The inserted plot shows the comparison between the real Ca_c and the Ca_{jump} at offset $= 0.08$.

with the viscosity ratio and scaled as $\lambda^{0.82}$. However, this dependence on the viscosity ratio is weaker than is predicted by the simple scaling arguments.

In the case of glancing collisions, the critical coalescence conditions were examined by changing the initial offset as well as the viscosity ratio. The critical capillary number for coalescence was found to decrease with increased offset for small offsets, but then increase with the further increase of the offset for all viscosity ratios greater than $O(0.1)$. This is in contrast to the decrease of the critical capillary number with increasing offset in the earlier study (Yang *et al.* 2001) at a viscosity ratio of 0.096. This is because the drops begin to coalesce in the extensional quadrant of the flow ($\phi > 45^\circ$) after the external flow starts to pull the drops apart. When the drops coalesce in the extensional quadrant at large offsets, the coalescence angle as a function of the capillary number changes: there is a discontinuous step change of the coalescence angle into the extensional quadrant and a continuous increase of the angle within the extensional quadrant, depending on the offset and viscosity ratio. The nipple formation appears to be the most convincing mechanism for coalescence in the extensional quadrant. The fact that coalescence with $\phi > 45^\circ$ occurs more readily for the higher viscosity ratio systems would seem to be qualitatively consistent with an explanation in terms of nipple formation in the thin-film region within the extensional quadrant. The dependence of the critical capillary number on the viscosity ratio did not follow the simple power-law dependence as predicted in the simple scaling theory ($Ca_c \sim \lambda^{-2/3}$). The scaling theory seems to be qualitatively flawed. There cannot be any such power-law dependence. The dependence is, in fact, wholly influenced by

the initial offset. However, the maximum offset for coalescence decreased with the viscosity ratio, as expected.

The data tell us that the evolution of the thin-film configurations during the drainage process is complicated for glancing collisions, and requires further study. Aspects of the experimental results which remain to be explained are indicative of the direction which further theoretical investigations of the coalescence process must take.

This work was supported by grants from the fluid mechanics program of the National Science Foundation, and the microgravity program of NASA.

REFERENCES

Abid, S. & Chesters, A. K. 1994 The drainage and rupture of partially-mobile films between colliding drops at constant approach velocity. *Intl J. Multiphase Flow* **20**, 613–629.

Baldessari, F. 2004 Theoretical studies of flow induced coalescence. PhD thesis, Chemical Engineering Depatment, Santa Barbara, University of California.

Bazhlekov, I. B., Chesters, A. K. & van de Vosse, F. N. 2000 The effect of the dispersed to continuous-phase viscosity ratio on film drainage between interacting drops. *Intl J. Multiphase Flow* **26**, 445–466.

Bentley, B. J. & Leal, L. G. 1986 A computer-controlled 4-roll mill for investigations of particle and drop dynamics in two-dimensional linear shear flows. *J. Fluid Mech.* **167** 219–240.

Burkhart, B. E., Gopalkrishnan, P. V., Hudson, S. D., Jamieson, A. M., Rother, M. A. & Davis, R. H. 2001 Droplet growth by coalescence in binary fluid mixtures. *Phys. Rev. Lett.* **8709**, art. 098304.

Chesters, A. K. 1991 The modeling of coalescence processes in fluid liquid dispersions – a review of current understanding. *Chem. Engng Res. Des.* **69**, 259–270.

Cristini, V., Blawzdziewicz, J. & Loewenberg, M. 2001 An adaptive mesh algorithm for evolving surfaces: simulations of drop breakup and coalescence. *J. Comput. Phys.* **168**, 445–463.

Goveas, J. L. & Fredrickson, G. H. 1998 Apparent slip at a polymer–polymer interface. *Eur. Phys. J.* B **2**, 79–92.

Goveas, J. L. & Fredrickson, G. H. 2000 Apparent slip at polymer–polymer interface *Eur. Phys. J.* B **13**, 201–201.

Guido, S. & Simeone, M. 1998 Binary collision of drops in simple shear flow by computer- assisted video optical microscopy. *J. Fluid Mech.* **357**, 1–20.

Ha, J. W., Yoon, Y. & Leal, L. G. 2003 The effect of compatibilizer on the coalescence of two drops in flow. *Phys. Fluids* **15**, 849–867.

Hu, Y. T., Pine, D. J. & Leal, L. G. 2000 Drop deformation, breakup, and coalescence with compatibilizer. *Phys. Fluids* **12**, 484–489.

Hudson, S. D., Jamieson, A. M. & Burkhart, B. E. 2003 The effect of surfactant on the efficiency of shear-induced drop coalescence. *J. Colloid Interface Sci.* **265**, 409–421.

Loewenberg, M. & Hinch, E. J. 1997 Collision of two deformable drops in shear flow. *J. Fluid Mech.* **338** 299–315.

Lyu, S. P., Bates, F. S. & Macosko, C. W. 2000 Coalescence in polymer blends during shearing. *AIChE J.* **46**, 229–238.

Manev, E., Scheludk, A. & Exerowa, D. 1974 Effect of surfactant concentration on critical thicknesses of liquid-films. *Colloid Polymer Sci.* **252**, 586–593.

Milner, S. T. & Xi, H. W. 1996 How copolymers promote mixing of immiscible homopolymers. *J. Rheol.* **40**, 663–687.

Mousa, H., Agterof, W. & Mellema, J. 2001 Experimental investigation of the orthokinetic coalescence efficiency of droplets in simple shear flow. *J. Colloid Interface Sci.* **240**, 340–348.

Park, C. C., Baldessari, F. & Leal, L. G. 2003 Study of molecular weight effects on coalescence: interface slip layer. *J. Rheol.* **47**, 911–942.

Ramic, A. J., Hudson, S. D., Jamieson, A. M. & Manas-Zloczower, I. 2000 Temporary droplet-size hysteresis in immiscible polymer blends. *Polymer* **41**, 6263–6270.

Rother, M. A., Zinchenko, A. Z. & Davis, R. H. 1997 Buoyancy-driven coalescence of slightly deformable drops. *J. Fluid Mech.* **346** 117–148.

Rother, M. A. & Davis, R. H. 2001 The effect of slight deformation on droplet coalescence in linear flows. *Phys. Fluids* **13**, 1178–1190.

Sharma, A. & Ruckenstein, E. 1987 Critical thickness and lifetimes of foams and emulsions – role of surface wave-induced thinning. *J. Colloid Interface Sci.* **119**, 14–29.

Sharma, A. & Ruckenstein, E. 1988 Effects of surfactants on wave-induced drainage of foam and emulsion films. *Colloid Polymer Sci.* **266**, 60–69.

Taylor, G. I. 1934 The formation of emulsions in definable fields of flow. *Proc. R. Soc. Lond.* A **146**, 501–523.

Tretheway, D. C., Muraoka, M. & Leal, L. G. 1999 Experimental trajectories of two drops in planar extensional flow. **11**, 971–981.

Vinckier, I., Moldenaers, P., Terracciano, A. M. & Grizzuti, N. 1998 Droplet size evolution during coalescence in semiconcentrated model blends. *AIChE J.* **44**, 951–958.

Wang, H., Zinchenko, A. Z. & Davis, R. H. 1994 The collision rate of small drops in linear flow-fields. *J. Fluid Mech.* **265**, 161–188.

Yang, H., Park, C. C., Hu, Y. T. & Leal, L. G. 2001 The coalescence of two equal-sized drops in a two-dimensional linear flow. *Phys. Fluids* **13**, 1087–1106.

Yeo, L. Y. & Matar, O. K. 2003 Hydrodynamic instability of a thin viscous film between two drops. *J. Colloid Interface Sci.* **261**, 575–579.

Zinchenko, A. Z., Rother, M. A. & Davis, R. H. 1997 A novel boundary-integral algorithm for viscous interaction of deformable drops. *Phys. Fluids* **9**, 1493–1511.